Silica-Supported Fe(II), Co(II) and Ni(II) Complexes as Efficient Catalysts to Esterification of Levulinic acid with Polyol

Md. Anwar Hossain[1,2,*,] and Lee Hwei Voon[2,]

[1]Department of Chemistry, Rajshahi University of Engineering & Technology, Rajshahi-6204, Bangladesh
[2]Nanotechnology & Catalysis Research Centre (Nanocat), Level 3, Block A, Institute for Advanced Studies, University of Malaya, Kuala Lumpur 50603, Malaysia

*Corresponding author: E-mail: anwarruet10@gmail.com

Biomass-derived feedstocks were used to synthesize a new polyol-based ester for biolubricant production to overcome the dependence on mineral oil. Although biomass-derived oil is a potential alternative to polyol ester, upgrading is inevitable before using it as a biolubricant. Levulinic acid (model acid), obtained from a bio oil, was used for the esterification of two polyols, for example, neopentyl glycol (NPG) and trimethylolpropane (TMP), in the presence of ligand metal Fe(II), Co(II), and Ni(II) complexes as catalyst. Silica-supported Fe(II), Co(II) and Ni(II) complexes *viz.* $[Fe(Tyr)(Amp)]Cl \cdot SiO_2$, $[Co(Phe)(Bpy)]Cl \cdot SiO_2$ and $[Ni(Leu)(Phen)]Cl \cdot SiO_2$ were synthesized by the reaction of ligands [L-phenylalanine (Phe), L-tyrosine (Tyr), L-leucine (Leu), 4,4′-bipyridine (Bpy), 2-aminopyridine (Amp) and 1,10-phenanthroline (Phen)] with respective metal(II) chloride salts. All the metal complexes were characterized by elemental analysis, magnetic susceptibility, TGA/DTA, FTIR, powder-XRD and SEM methods. The catalytic activities of the complexes were further investigated *via* esterification of two polyols (*e.g.* neopentyl glycol and trimethylolpropane) by biomass-derived levulinic acid (LA). Herein, iron(II) complex was found to be more active, demonstrating its better efficiency as a catalyst towards the esterification of levulinic acid for synthesizing ester-based oils.

Keywords: Biomass, Esterification, Ligand-metal complexes, Ester-based oils, Supported metal complexes.

INTRODUCTION

One of the significant alternatives to petroleum currently used in industries is biomass, which is a renewable, distinct carbon resource for the preparation of biolubricants and useful chemicals. Biomass (*i.e.* wood, straw, corn, grass, soybean, and algae), through pyrolysis or hydrotreating, produces many organic compounds, including bio-oil and biochar [1,2]. This bio-oil contains nearly 400 organic chemicals, including carboxylic acids, for example, acetic, propionic, butanoic acid and levulinic acid. Levulinic acid (model acid), *i.e.*, 4-oxo-pentanoic acid, having five carbon atoms with ketone and carboxyl functional groups, can be obtained from starch, glucose, fructose, and lignocellulosic residues [3,4]. This acid has been given the top position among chemicals by the U.S. Department of Energy and is considered one of the most attractive chemicals derived from biomass based feedstocks [5]. Furthermore,

4-oxopentanoic acid can easily react with polyols, for example, neopentyl glycol (NPG), trimethylolpropane (TMP) and penta-erythritol (PE), in the presence of Lewis acid catalysts to produce levulinate esters. These ester-based oils are usually used in lubricant formulations, fragrant chemicals, green solvents, energy resources, plasticizers and perfumes [6]. Therefore, NPG and TMP levulinate esters are synthesized as they have similar lubricant properties, viscosity index, flash point, pour point, and biodegradability. Thus, there are immense applications for levulinic acid to produce biolubricants than vegetable oils in economic aspects.

The reduction of unsaturated esters using catalyst to highly stable hydrocarbon based esters is most important reactions in organic chemistry. Several catalysts have been used effectively in esterification processes using homogenous and heterogeneous catalysts, *e.g.* silica supported Mn(II), Co(II), Ni(II) and Cu(II) Schiff base complexes, vinyl(IV) complexes, Mn(III)

and Co(III) salen complexes [7] and Mn(III) and Fe(III) Schiff base complexes [8].

Reduction of esters using homogeneous catalysts has been comparatively less examined and is limited to activate esters only. On the other hand, heterogeneous catalysts have been widely used in the reduction of esters [9]. The applications of transition metal complexes have attained great attention in the last few years due to their ability to act as catalyst or catalyst precursor. The thermal stability and tenability of ligand complexes make them actually suitable for a wide range of catalytic and stoichiometric conversions [10].

The simplest pathway to transform a homogeneous catalyst into a heterogamous catalyst [11] comprises of immobilization or encapsulation [11,12] of active metal complexes onto a solid support [13]. Metal complexes anchoring on the surface of mesoporous silica is one of the most popular methods in recent years. The metal complexes tethered on the mesoporous silica exhibit significant catalytic activities due to the increased dispersion of active sites and rapid diffusion of large organic molecules [14]. The anchoring of metal complexes on the surface of mesoporous silica is one of the most popular methods in recent years. The metal complexes tethered on the mesoporous silica exhibit significant catalytic activities due to the increased dispersion of the active sites and the faster diffusion of large organic molecules [15]. In addition, the impregnation method eases catalyst stability and selectivity towards organic reactions [16]. Many methods have been used for grafting of organometallic complexes onto solid inorganic support, including ion pairing and encapsulation [17], physisorption and covalent ligand binding [18]. Thus, the strong interactions between the metal and the ligand generate significant stability for this kind of catalyst, which allows them to be reused in several cycles without losing their efficiency [15].

These studies stated the methods of immobilizing organometallic complexes on a solid support, including inorganic porous material (*e.g.* silica, alumina, silica-alumina, SBA-15, MCM-41, MCM-48) [15,19-22] and functional organic polymers [11,20,23]. A mesoporous silica support material seems to be most useful and versatile solids for immobilization of organometallic complexes [12,24,25]. Considering these facts, the

authors have selected acidic silica as a support material for grafting of organometallic complexes [22]. However, this structural integrity promotes the uniform loading of organometallic complexes onto the solid supports and facilitates catalytic activity of the reaction substrates [14].

EXPERIMENTAL

All chemicals and solvents in the study were of analytical grade and used without further purification. L-phenylalanine, L-tyrosine, 2-aminopyridine and L-leucine were obtained from Sigma-Aldrich (USA), whereas 1,10-phenanthroline and 4,4′-bipyridine were purchased from Merck (India). The metal salts *viz.* Fe(II), Co(II) and Ni(II) chlorides were obtained from Fluka Chemicals (Switzerland). For esterification reactions, levulinic acid and polyols, for example, neopentyl glycol (NPG) and trimethylolpropane (TMP) were obtained from Merck.

Physical measurements: Fourier-transform infrared spectroscopy (FTIR) analyses were performed at 4000-400 cm^{-1} range with pressed KBr pellets by using an IR-8400/8900 Shimadzu spectrophotometry. Magnetic susceptibility was measured using a magnetic susceptibility balance (Sherwood Scientific, UK). The elemental analysis (carbon, hydrogen and nitrogen) and metals were recorded using a Yanaco CHN-corder-MT-5. The physical structure of catalysts, compositional analysis and surface morphology were determined through scanning electron microscopy (SEM) (JEOL, JSM-6360 LV) coupled with energy-dispersive X-ray spectroscopy (EDS) (JEOL, JED-2300). The thermal decomposition behaviour of residual hydrocarbons on the spent catalysts was determined using thermogravimetric and differential thermal analysis (TGA/DTA 60, Shimadzu) at a heating rate of 10 ºC min^{-1} from the room temperature to 800 ºC under nitrogen flow. Powder X-ray diffraction (XRD) analysis was obtained using Rigaku RINT 2200 equipment with Cu$K\alpha$ radiation operated at 40 kV and 40 mA. Data were collected at a 2θ range of 10º-90º and the phases were identified based on matching experimental patterns to entries in the version 6.0 indexing HighScore Plus software.

Synthesis of silica supported metal(II) complexes: The synthesis of complexes was followed by the following reaction (**Scheme-I**). The reaction with SiO$_2$ at 40-50 ºC for 10 h resulted
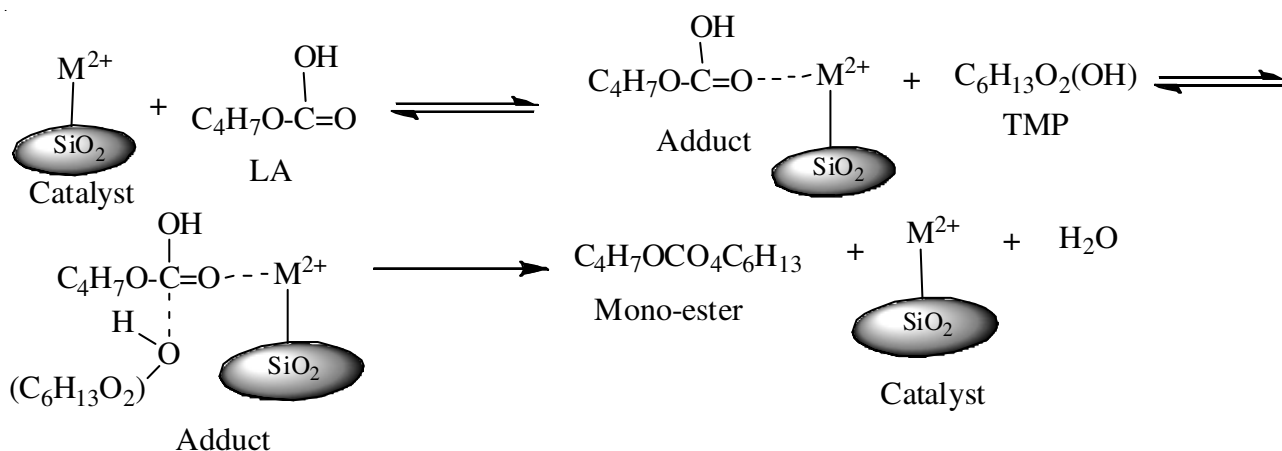
Scheme-I: Proposed route for the mono-esterification of levulinic acid (LA) with trimethylolpropane (TMP) catalyzed by silica-supported metal cation

in the formation of silica-supported Fe(II), Co(II) and Ni(II) complexes [22,26].

Synthesis of [Fe(Tyr)(Amp)]Cl·SiO₂: This complex was synthesized with a water:methanol (1:3) solution of 2-aminopyridine (1 mmol) and L-tyrosine (1 mmol) which was deprotonated prior by NaOH (0.05 mmol), to the iron(II) chloride solution (1 mmol) in methanol-water solution and stirred at 70-80 ºC for 2 h [9]. Upon cooling the solution, a green powdered compound obtained was filtered, washed with methanol, dried under vacuum condition and purified by recrystallization. Selected IR bands (KBr pellet, cm⁻¹): 3338, 3321, 2943, 1591, 1573, 1445, 1356, 1347, 1243, 1053, 531 and 495. Magnetic susceptibility; μ_{eff} = 3.71 (diamagnetic).

A solution of [Fe(Tyr)(Amp)]Cl in CH₃OH was added to a suspension of SiO₂ in methanol at a ratio of 1:6. The resulting suspension was heated and stirred at 40-50 ºC for 10 h. The greenish solid was filtered and then washed with methanol. The [Fe(Tyr)(Amp)]Cl·SiO₂ catalyst was dried at 60 ºC under vacuum overnight prior to use. Selected IR bands (KBr pellet, cm⁻¹): 3510, 3131, 2847, 1586, 1574, 1446, 1353, 1353, 1250, 1055, 528 and 491. EDX (metal content) (%): Fe, 6.882; Si, 93.116.

Synthesis of [Co(Phe)(Bpy)]Cl·SiO₂: The same procedure for the synthesis of [Co(Phe)(Bpy)]Cl·SiO₂ was repeated by substituting 2-aminopyridine and L-tyrosine with L-phenylalanine and 4,4′-bipyridine and Fe(II) metal center with Co(II). The violet solid was obtained on slow evaporation of the concentrated solution. Selected IR bands (KBr pellet, cm⁻¹): 3348, 3157, 3131, 2942, 1605, 1568, 1441, 1353, 1236, 1080, 545 and 487. Magnetic susceptibility; μ_{eff} = 4.39 (paramagnetic).

Silica powder was added to a solution of Co(Phe)(Bpy)]Cl in methanol (1:6) and heated at 40-50 ºC for 10 h with constant stirring. The solid was filtered, washed with methanol and dried at 60 ºC. Selected IR bands (KBr pellet, cm⁻¹): 3503, 3135, 2941, 1603, 1565, 1351, 1234, 1080, 548 and 485. EDX (metal content) (%): Co, 7.75; Si, 92.25.

Synthesis of [Ni(Leu)(Phen)]Cl·SiO₂: The method for synthesizing [Ni(Leu)(Phen)]Cl was repeated by substituting Co(II) salt with Ni(II) and L-phenylalanine and 4,4′-bipyridine with L-leucine and 1,10-phenanthroline. The green solid obtained on slow evaporation of concentrated solution was suitable for powder X-ray diffraction. Selected IR (KBr pellet, cm⁻¹): 3327, 3143, 2945, 1598, 1571, 1358, 1448, 1243, 1052, 530 and 495. Magnetic susceptibility; μ_{eff} = 3.24 (diamagnetic).

Porous silica was added to the solution of [Ni(Leu)(Phen)]-Cl in methanol (1:6) and heated at 40-50 ºC for 10 h with constant stirring. The solid compound was filtered, washed with methanol and dried at 60 ºC. Selected IR data (KBr pellet, cm⁻¹): 3507, 3327, 2951, 1592, 1573, 1451, 1035, 538 and 492. EDX (metal content) (%): Ni, 5.88; Si, 94.12.

Experimental for catalytic activity

Esterification: Catalytic activities were measured using the esterification reaction of the model acid (levulinic acid) with polyols (*i.e.* NPG and TMP) at 100-120 ºC in a silicone oil bath under a reflux condition as described earlier. [27]. After ending each reaction, the products were collected and analyzed by Gas Chromatography-Mass Spectrometer (Shimadzu-QP

5000) equipped with RTX-5-MS column (30 m × 0.25 mm × 0.25 µm) in split mode. The fraction peaks that collected from mass spectra were identified by the National Institute of Standards and Testing (NIST) library matching. Additionally, the catalytic activity of the complexes towards esterification (total product yield and product selectivity) (eqns. 1 and 2) [28] was determined by comparing the peak area % of the obtained spectra. To confirm the reproducibility of the results, the experiments were conducted three times, where average of the peak area and peak area % was calculated.

$$\text{Product yield (\%)} = \frac{\text{Total area of product} - \text{Area of reactant}}{\text{Total area of product}} \times 100 \quad (1)$$

$$\text{Product selectivity (\%)} = \frac{\text{Area of desired product}}{\text{Total area of product}} \times 100 \quad (2)$$

RESULTS AND DISCUSSION

The complexes [Fe(Tyr)(Amp)]Cl·SiO₂, [Co(Phe)(Bpy)]Cl·SiO₂ and [Ni(Leu)(Phen)]Cl·SiO₂ were successfully synthesized by reacting with Fe(II), Co(II) and Ni(II) chlorides with bidentate ligands as mixed ligands in water-methanol solution at 70-80 ºC. Afterwards, the complexes were impregnated with solid inorganic supports (silica) to prepare tethered complexes [7].

IR studies: The solid state IR spectra of the mixed ligand metal complexes with or without immobilization on inorganic silica support were in the range of 4000-400 cm⁻¹ (Fig. 1). The absorption peaks at 2935-2873 cm⁻¹ were attributed to the C-H stretching frequency in methylene groups of the complexes [13], while in impregnated molecules, the peaks disappeared. The spectra of porous silica showed a broad band at 3550-3250 cm⁻¹ assigned to the hydroxyl vibration of the hydrogen bonded internal silica groups. A sharp peak at 1081-1060 cm⁻¹ can be attributed to silanol-OH groups stretches and Si-O-Si bonds in the spectrum of all supported metal(II) complexes. Moreover, the presence of weak bands at around 3310 cm⁻¹ in the NH₂-M molecule was attributed to the N-H stretching of amino groups [8]. After grafting with silica, the band due to N-H vibration disappeared with the formation of a new band at 1645 cm⁻¹, assigned to the vibration of C-N band, which indicated the participation of amino ligands in bonding with the metal ions. The peaks at 495-477 cm⁻¹ and 597-562 cm⁻¹ were assigned to M-N and M-O stretching, respectively in the complexes [8,29].

Powder X-ray diffraction studies: The powder XRD spectra for [Fe(Tyr)(Amp)]Cl and [Fe(Tyr)(Amp)]Cl·SiO₂, [Co(Phe)(Bpy)]Cl and [Co(Phe)(Bpy)]Cl·SiO₂ and [Ni(Leu)-(Phen)]Cl·SiO₂ and [Ni(Leu)(Phen)]Cl·SiO₂ are shown in Fig. 2. The interplanar *d*-spacing values were measured from the diffractogram of the metal(II) complexes. Moreover, the Miller indices values were also determined to each *d*-spacing along with 2θ angles. The observed results implied that [Fe(Tyr)(Amp)]Cl belonged to the monoclinic crystal system of space group *C* 12, having unit cell parameters of a = 22.55 Å, b = 14.25 Å and c = 18.75 Å; and α = 90º, β = 112º and γ = 90º at the wavelength of 1.540598 Å. For [Co(Phe)(Bpy)]Cl, results also revealed the monoclinic crystal system of space group *C* 12 of unit cell
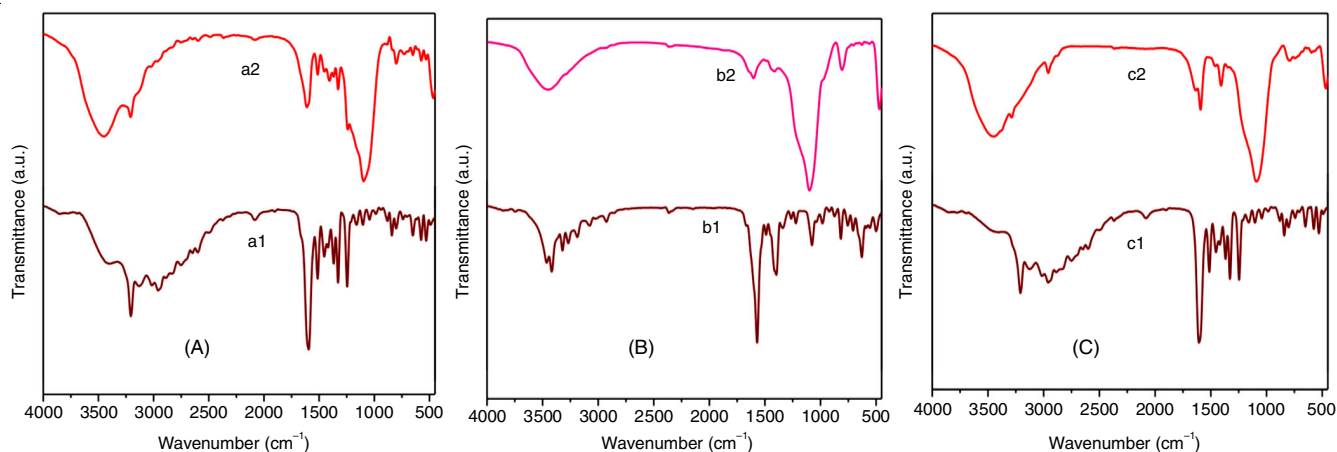
Fig. 1. FTIR spectra of (a1) [Fe(Tyr)(Amp)]Cl and (a2) [Fe(Tyr)(Amp)]Cl·SiO₂ (A), (b1) [Co(Phe)(Bpy)]Cl and (b2) [Co(Phe)(Bpy)]Cl·SiO₂ (B) and (c1) [Ni(Leu)(Phen)]Cl and (c2) [Ni(Leu)(Phen)]Cl·SiO₂ (C)
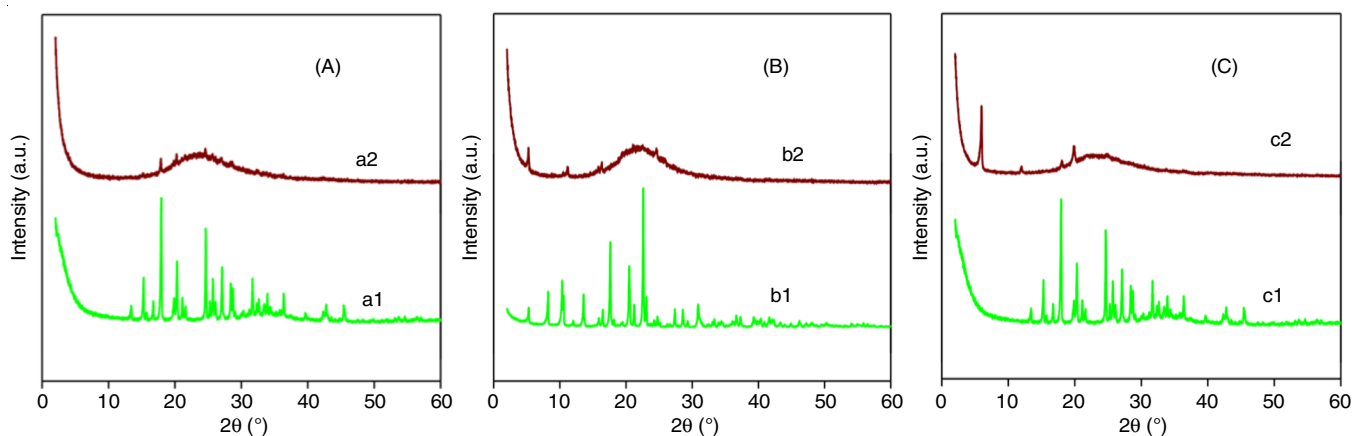

Fig. 2. Powder XRD patterns for (a1) [Fe(Tyr)(Amp)]Cl and (a2) [Fe(Tyr)(Amp)]Cl·SiO₂ (A), (b1) [Co(Phe)(Bpy)]Cl and (b2) [Co(Phe)(Bpy)]Cl·SiO₂ (B) and (c1) [Ni(Leu)(Phen)]Cl and (c2) [Ni(Leu)(Phen)]Cl·SiO₂ (C)

parameters with a = 8.13 Å, b = 10.55 Å, c = 13.95 Å; and α = 90º, β = 110º and γ = 90º. For complex [Ni(Leu)(Phen)]Cl, space group P 21 of unit cell parameters a = 12.72 Å, b = 15.35 Å, c = 12.78 Å; and α = 90º, β = 103º and γ = 90º at the wavelength of 1.540598 Å with maximum deviation of 2θ = 0.025º, implied that the ligand metal complexes were crystalline [30]. However, ligand metal complexes immobilized onto silica exhibited a sharp diffraction peak at around 2θ = 2.5º, corres-

ponding to the (1 0 0) reflection of hexagonal amorphous silica lattices [31]. Additionally, low intensity peaks of silica phases were found at (2θ = 15º to 40º) due to (1 1 0), (2 0 0) and (2 0 0) reflections, which indicated that the metal complexes were uniformly immobilized within the silica matrix [18].

Thermal studies: Thermal properties of the metal(II) complexes and their corresponding silica-tethered complexes were examined by using thermogravimetric analysis (TGA).
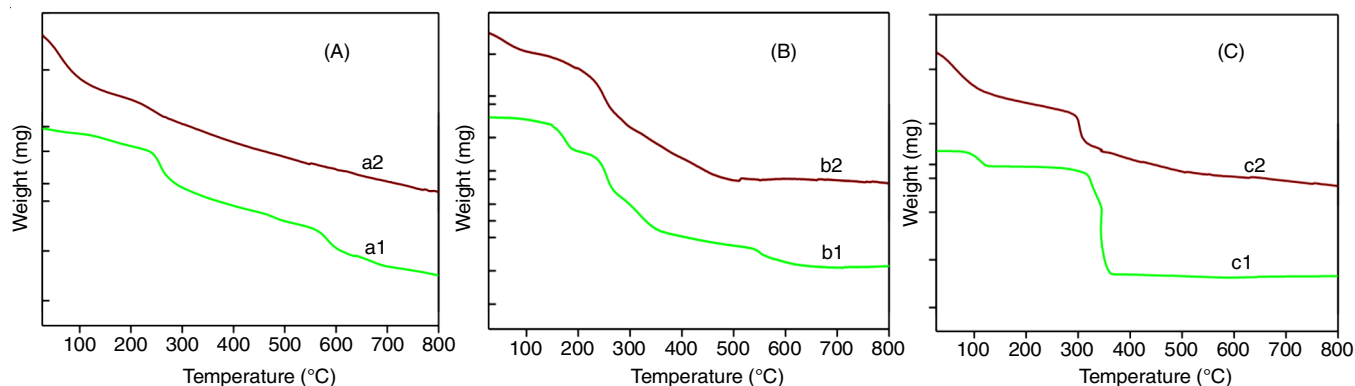

Fig. 3. TGA curves for (a1) [Fe(Tyr)(Amp)]Cl and (a2) [Fe(Tyr)(Amp)]Cl·SiO₂ (A), (b1) [Co(Phe)(Bpy)]Cl and (b2) [Co(Phe)(Bpy)]Cl·SiO₂ (B) and (c1) [Ni(Leu)(Phen)]Cl and (c2) [Ni(Leu)(Phen)]Cl·SiO₂ (C)

The thermogravimetric curves (Fig. 3) showed that both homo-geneous and heterogeneous metal complexes were thermally stable. Generally, metal complexes had four endothermic peaks in the thermogravimetric curves. Physically adsorbed water molecules present in the metal(II) complexes were eliminated at 50 to 90 ºC with an endothermic peak in the thermogravi-metric curves of complexes. The elimination of coordinated water and solvent molecules [7] from the metal complexes were determined at 100 to 240 ºC. The peaks at about 260 to 350 ºC were the degradations of coordinated chloride ions and one ligand group. The highest peaks were attributed between 400 to 800 ºC when the elimination of another ligand group occurred and finally metal oxides formed. In general, ligand groups with lower molecular masses were eliminated first, followed by the ligands with higher molecular masses [32]. The same degrada-tion patterns were also observed for all three impregnated comp-lexes, where there was gradual weight loss followed by their corresponding complexes and finally metal oxide formed [33]. The silica-supported mixed ligands do not allow a 1:2 ratio for metal-ligand complexation due to bulky structure of silica [34].

SEM study: The SEM images were obtained to observe the surface morphology and physical structures of the metal(II) complexes before and after impregnation. The morphological differences between metal(II) complexes and silica-supported complexes in SEM images exhibited an important proof of loading of the complexes onto the silica particles [13,35]. These micrographs also displayed a wide extent of shapes and particle sizes after immobilization. Metal(II) complexes diffused on the SiO_2 mesoporous channels that fitted perfectly with the pores. In general, the SEM micrographs displayed single-phage form-ation with well-defined, grain-like shapes which were particles sized in the range of 0.5 µm. Moreover, different characteristic

shapes of samples were identified, these SEM images were fairly different from other complexes. Additionally, the well-dispersed silica-supported Fe(II), Co(II) and Ni(II) complexes exhibited strong catalytic activity since they had large surface areas on the silica particles and had cavities as an internal and external surface (Fig. 4) [36]. Indeed, the EDX results also confirmed that metal cations were well-dispersed on silica-supported complexes [13].

Catalytic activity study

Esterification: The catalytic performances of the metal complexes were determined *via* esterification reactions of levulinic acid with polyols, which are neopentyl glycol (NPG) and trimethylolpropane (TMP) (Table-1). Prior investigating the activity of complexes, preparatory studies using sulphuric acid as a liquid acid catalyst were accomplished similar to literature method [27]. The reaction temperature was optimized at 105 and 115 ºC for NPG and TMP esterification based on the ester yield and selectivity. The reaction time of 2 h and catalyst loading of 2 wt.% with respect to levulinic acid were also optimized.

The esterification of levulinic acid with TMP produced higher yields compared to NPG for all the metal (II) complexes. Trimethylolpropane had three (-OH) functional groups prod-ucing in LA-mono, LA-di and LA-triesters. On the other hand, neopentyl glycol had two alcoholic groups and was less active, forming LA-mono, LA-diester was detected. For comparing the performances of these catalysts, similar reactions were performed using H_2SO_4 as a catalyst [37] and observed silica-tethered complexes (Table-2) had more activity than H_2SO_4.

This study also revealed that the mixed ligand complexes that impregnated with porous silica were highly potential for
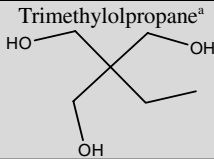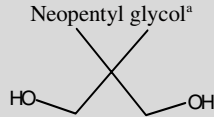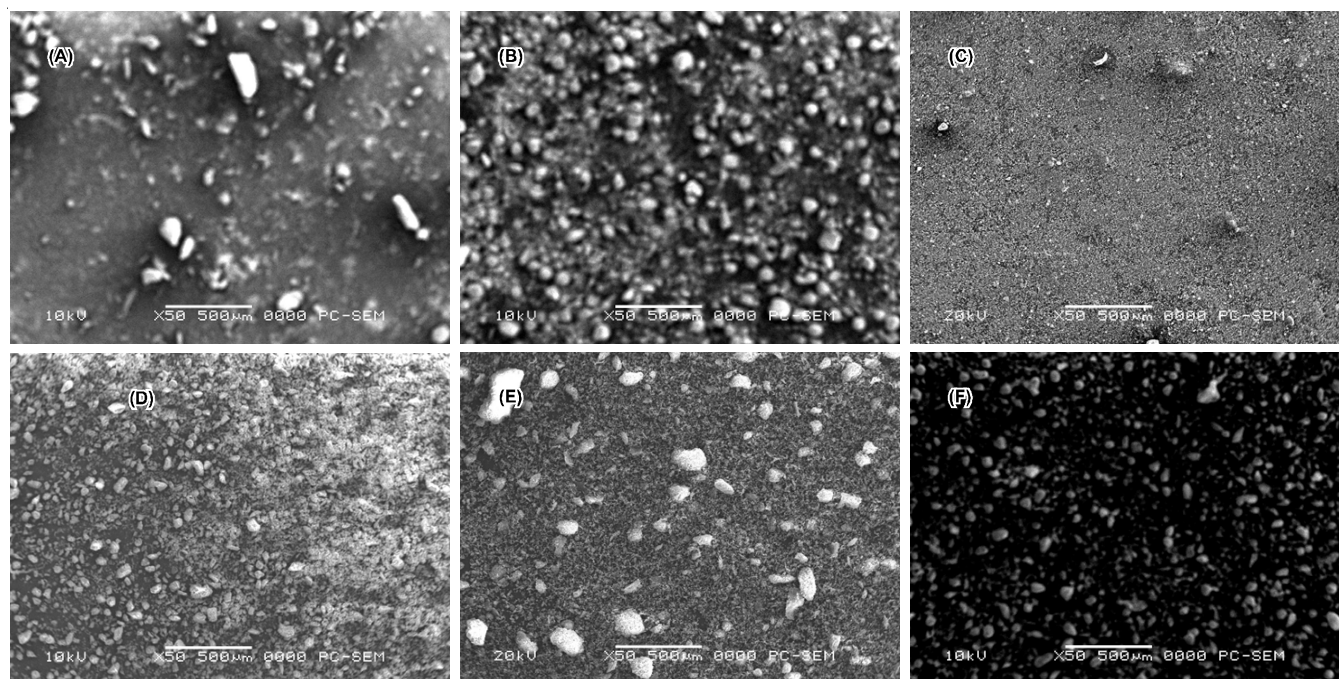
Fig. 4. The SEM images of [Fe(Tyr)(Amp)]Cl (A) and [Fe(Tyr)(Amp)]Cl·SiO_2 (B), [Co(Phe)(Bpy)]Cl (C) and [Co(Phe)(Bpy)]Cl·SiO_2 (D) and [Ni(Leu)(Phen)]Cl (E) and [Ni(Leu)(Phen)]Cl·SiO_2 (F) at X50 magnification

TABLE-1
ESTERIFICATION OF LEVULINIC ACID WITH (TMP) AND (NPG) OVER
Fe(II), Co(II) AND Ni(II) COMPLEXES, H$_2$SO$_4$ AND WITHOUT CATALYST

Polyols	Catalysts	Ester yield (%)[b]		
		Mono	Di	Tri
Trimethylolpropane[a]	[Fe(Tyr)(Amp)]Cl	58.27	8.35	10.78
	[Co(Phe)(Bpy)]Cl	55.96	10.14	5.13
	[Ni(Leu)(Phen)]Cl	49.24	7.49	4.68
	H$_2$SO$_4$	52.00	15.25	1.58
	Blank experiment	15.76	3.00	0.95
Neopentyl glycol[a]	[Fe(Tyr)(Amp)]Cl	60.38	10.24	–
	[Co(Phe)(Bpy)]Cl	54.23	7.88	–
	[Ni(Leu)(Phen)]Cl	50.21	8.15	–
	H$_2$SO$_4$	51.00	15.00	–
	Blank experiment	9.75	2.50	–

[a]Reaction conditions: Catalyst loading = 2% w/w of LA; LA: TMP = 3:1 at 115 °C, LA: NPG = 2:1 at 105 °C; reaction time = 2 h
[b]Calculated using eqn. 1

TABLE-2
ESTERIFICATION OF LEVULINIC ACID WITH (TMP)
AND (NPG) OVER SILICA-SUPPORTED Fe(II),
Co(II) AND Ni(II) COMPLEXES

Polyols	Catalysts	Ester yield (%)[b]		
		Mono	Di	Tri
TMP[a]	[Fe(Tyr)(Amp)]Cl·SiO$_2$	32.81	38.10	8.85
	[Co(Phe)(Bpy)]Cl·SiO$_2$	23.55	45.14	5.55
	[Ni(Leu)(Phen)]Cl·SiO$_2$	21.85	44.14	4.24
NPG[a]	[Fe(Tyr)(Amp)]Cl·SiO$_2$	32.28	45.23	–
	[Co(Phe)(Bpy)]Cl·SiO$_2$	27.76	40.84	–
	[Ni(Leu)(Phen)]Cl·SiO$_2$	30.55	36.73	–

[a]Reaction conditions: Catalyst loading = 2% w/w of LA; LA: TMP = 3:1 at 115 °C, LA: NPG = 2:1 at 105 °C, reaction time = 2 h (reflux condition); [b]Calculated using eqn. 1

esterification of levulinic acid with NPG and TMP, produced higher quantity of levulinate-di and levulinate-tri esters compared to their corresponding metal complexes. This might possibly due to complete immobilization of metal complexes onto silica support which produced more Lewis acidic sites and so produced more LA-di and LA-tri esters. However, Lewis acidity of the immobilized complexes without protons and the resulting catalytic activity is due to interaction with catalyst metal ion and faster diffusion of large organic molecules [15] as shown in **Scheme-I**.

Masood *et al.* [38] explained the scope of Ca-methoxide heterogeneous catalyst to these catalytic reactions. However, efficient catalyst purification methods are still necessary as there is metallic soap formation tendency with catalyst to the fatty acids. Therefore, impregnated complex catalysts in the present study were highly active and selective towards lubricant base oil production. Finally, esterification reaction revealed that the most active homogenous catalyst was [[Fe(Tyr)(Amp)]Cl, which yielded 77.40% LA-TMP ester and 70.62% LA-NPG ester. Among the homogeneous complexes, Fe(II) complex exhibited highest activity with majority of LA-triesters. Finally, the most active silica-supported metal(II) complex was [Fe(Tyr)-(Amp)]Cl·SiO$_2$, which yielded 79.76% LA-TMP and 77.51% LA-NPG ester. All the supported metal(II) complexes, Fe(II) complex after tethered with porous silica support generate more

acidic sites, which favoured for the LA-di and LA-triesters products.

Conclusion

In summary, two polyol esters were synthesized (*i.e.* LA-NPG and LA-TMP ester) effectively using bio-oil model acid (levulinic acid) with the help of organometallic complexes as catalyst. In this study, biomass derived oil was supposed as acid feedstock where levulinic acid was obtained as a major ingredient. These polyol based esters synthesized from non-food feedstocks by esterification have important applications as lubricant base oil. Furthermore, the catalytic performances of the metal complexes were measured *via* esterification reaction of levulinic acid with neopentyl glycol (NPG) and trimethyl-olpropane (TMP). The analytical results indicated that the most active homogenous catalyst is [[Fe(Tyr)(Amp)]Cl, which yields 77.40% LA-TMP and 70.62% LA-NPG ester, respectively. On the other hand, the most active silica-supported complex was [[Fe(Tyr)(Amp)]Cl·SiO$_2$ which rendered 79.76% LA-TMP and 77.51% LA-NPG ester, respectively. Among the Ni(II), Co(II), Fe(II) complexes, Fe(II) was more active on the basis of levulinic acid conversion. Thus, it might be concluded that iron(II) complexes have maximum catalytic performance.

CONFLICT OF INTEREST

The authors declare that there is no conflict of interests regarding the publication of this article.

REFERENCES

1. M.I. Jahirul, M.G. Rasul, A.A. Chowdhury and N. Ashwath, *Energies*, **5**, 4952 (2012);
https://doi.org/10.3390/en5124952

2. P. Gallezot, *Chem. Soc. Rev.*, **41**, 1538 (2012);
https://doi.org/10.1039/C1CS15147A

3. A. Pawar, N.L. Panwar and B.L. Salvi, *J. Mater. Cycles Waste Manag.*, **22**, 1712 (2020);
https://doi.org/10.1007/s10163-020-01063-w

4. K.Y. Nandiwale and V.V. Bokade, *Process Saf. Environ. Prot.*, **99**, 159 (2016);
https://doi.org/10.1016/j.psep.2015.11.003

5. M.A. Hossain, M.A. Mohamed Iqbal, N.M. Julkapli, P.S. Kong, J.J. Ching and H.V. Lee, *RSC Adv.*, **8**, 5559 (2018);
https://doi.org/10.1039/C7RA11824D

6. E.K. Heikal, M.S. Elmelawy, S.A. Khalil and N.M. Elbasuny, *Egypt. J. Petroleum*, **26**, 53 (2017);
https://doi.org/10.1016/j.ejpe.2016.03.003

7. Y. Yang, Y. Zhang, S. Hao and Q. Kan, *Chem. Eng. J.*, **171**, 1356 (2011);
https://doi.org/10.1016/j.cej.2011.05.047

8. M. Ozdemir, *Inorg. Chim.Acta*, **421**, 1 (2014);
https://doi.org/10.1016/j.ica.2014.05.024

9. M.A. Hossain, C.L.Y. Lian, M. Al-Amin A.A. Islam, M.C. Sheikh, J.J. Ching and L.H. Voon, *BioResources*, **13**, 5512 (2018).

10. K.C. Gupta and A.K. Sutar, *Coord. Chem. Rev.*, **252**, 1420 (2008);
https://doi.org/10.1016/j.ccr.2007.09.005

11. Anuradha, S. Kumari, S. Layek and D.D. Pathak, *J. Mol. Struct.*, **1130**, 368 (2017);
https://doi.org/10.1016/j.molstruc.2016.10.053

12. K. Mori and H. Yamashita, Silica-Supported Metal Complex Photo-catalysts, In: Nanostructured Photocatalysts, Springer, pp. 465-477 (2016).

13. S. Urus, H. Adigüzel and M. Incesu, *Chem. Eng. J.*, **296**, 90 (2016);
https://doi.org/10.1016/j.cej.2016.03.101

14. M. Zendehdel, F. Zamani and H. Khanmohamadi, *Micropor. Mesopor. Mater.*, **225**, 552 (2016);
https://doi.org/10.1016/j.micromeso.2016.01.042

15. F. Habeche, M. Hachemaoui, A. Mokhtar, K. Chikh, F. Benali, A. Mekki, F. Zaoui, Z. Cherifi and B. Boukoussa, *J. Inorg. Organometal. Polym. Mater.*, **30**, 4245 (2020);
https://doi.org/10.1007/s10904-020-01689-1

16. B. Tamami, F. Farjadian, S. Ghasemi, H. Allahyaria and M. Mirzadeh, *J. Braz. Chem. Soc.*, **26**, 1591 (2015);
https://doi.org/10.5935/0103-5053.20150129

17. E. Ispir, *Phosphorus Sulfur Silicon Rel. Elem.*, **189**, 1644 (2014);
https://doi.org/10.1080/10426507.2014.885971

18. D.D. Van, T. Hosokawa, M. Saito, Y. Horiuchi and M. Matsuoka, *Appl. Catal. A Gen.*, **503**, 203 (2015);
https://doi.org/10.1016/j.apcata.2015.05.039

19. H. Pan, J. Wang, L. Chen, G. Su, J. Cui, D. Meng and X. Wu, *Catal. Commun.*, **35**, 27 (2013);
https://doi.org/10.1016/j.catcom.2013.02.007

20. M.A. Goni, E. Rosenberg, S. Meregude and G. Abbott, *J. Organomet. Chem.*, **807**, 1 (2016);
https://doi.org/10.1016/j.jorganchem.2016.01.032

21. B. Lai, Z. Huang, Z. Jia, R. Bai and Y. Gu, *Catal. Sci. Technol.*, **6**, 1810 (2016);
https://doi.org/10.1039/C5CY01012H

22. D. Zois, C. Vartzouma, Y. Deligiannakis, N. Hadjiliadis, L. Casella, E. Monzani and M. Louloudi, *J. Mol. Catal. Chem.*, **261**, 306 (2007);
https://doi.org/10.1016/j.molcata.2006.11.023

23. B. Tamami and S. Ghasemi, *J. Organomet. Chem.*, **794**, 311 (2015);
https://doi.org/10.1016/j.jorganchem.2015.05.041

24. Y. Kuwahara, Y. Magatani and H. Yamashita, *Catal. Today*, **258**, 262 (2015);
https://doi.org/10.1016/j.cattod.2015.01.015

25. J.W. Comerford, S.J. Hart, M. North and A.C. Whitwood, *Catal. Sci. Technol.*, **6**, 4824 (2016);
https://doi.org/10.1039/C6CY00134C

26. M. Salavati-Niasari and A. Amiri, *Appl. Catal. A Gen.*, **290**, 46 (2005);
https://doi.org/10.1016/j.apcata.2005.05.009

27. M.A. Hossain, C.Y.L. Low, C.M. Sheikh, J.C. Juan and H.V. Lee, *J. Mol. Struct.*, **1175**, 566 (2019);
https://doi.org/10.1016/j.molstruc.2018.08.011

28. C.-L.Y. Lian, L.H. Voon and S.A. Hamid, *Malaysian J. Catal.*, **2**, 46 (2017).

29. A.A. Alshaheri, M.I.M. Tahir, M.B.A. Rahman, T.B.S.A. Ravoof and T.A. Saleh, *Chem. Eng. J.*, **327**, 423 (2017);
https://doi.org/10.1016/j.cej.2017.06.116

30. A. Puškaric, I. Halasz, M. Gredièak, A. Palèic and J. Bronic, *New J. Chem.*, **40**, 4252 (2016);
https://doi.org/10.1039/C5NJ03001C

31. M.R. Didgikar, D. Roy, S.P. Gupte, S.S. Joshi and R.V. Chaudhari, *Ind. Eng. Chem. Res.*, **49**, 1027 (2010);
https://doi.org/10.1021/ie9007024

32. N. Xing, L.T. Xu, F.Y. Bai, H. Shan, Y.H. Xing and Z. Shi, *Inorg. Chim. Acta*, **409**, 360 (2014);
https://doi.org/10.1016/j.ica.2013.09.004

33. H.R. Dholariya, K.S. Patel, J.C. Patel and K.D. Patel, *Spectrochim. Acta A Mol. Biomol. Spectrosc.*, **108**, 319 (2013);
https://doi.org/10.1016/j.saa.2012.09.096

34. A.N. Kursunlu, E. Guler, H. Dumrul, O. Kocyigit and I.H. Gubbuk, *Appl. Surf. Sci.*, **255**, 8798 (2009);
https://doi.org/10.1016/j.apsusc.2009.06.055

35. S. Urus, M. Dolaz and M. Tümer, *J. Inorg. Organomet. Polym. Mater.*, **20**, 706 (2010);
https://doi.org/10.1007/s10904-010-9394-1

36. M. Islam, P. Mondal, S. Mondal, S. Mukherjee, A.S. Roy, M. Mubarak and M. Paul, *J. Inorg. Organomet. Polym. Mater.*, **20**, 87 (2010);
https://doi.org/10.1007/s10904-009-9310-8

37. H. Ji, B. Wang, X. Zhang and T. Tan, *RSC Adv.*, **5**, 100443 (2015);
https://doi.org/10.1039/C5RA14366G

38. H. Masood, R. Yunus, T.S.Y. Choong, U. Rashid and Y.H. Taufiq Yap, *Appl. Catal. A Gen.*, **425-426**, 184 (2012);
https://doi.org/10.1016/j.apcata.2012.03.019